Journal of Applied Polymer Science

Melt Spinning of Conductive Textile Fibers with Hybridized Graphite Nanoplatelets and Carbon Black Filler

Erik Nilsson,[1,2] Henrik Oxfall,[2] Wojciech Wandelt,[1] Rodney Rychwalski,[2] Bengt Hagström[1,2]

[1]Swerea IVF, Textiles and Plastics Department, Box 104, SE-431 22 Mölndal, Sweden

[2]Department of Materials and Manufacturing Technology, Chalmers University of Technology, 412 96 Göteborg, Sweden

Correspondence to: B. Hagström (E-mail: bengt.hagstrom@swerea.se).

ABSTRACT: In this study, two different carbon fillers: carbon black (CB) and graphite nanoplatelets (GNP) are studied as conductive fillers for the preparation of conductive polypropylene (PP) nanocomposites. In order to obtain a homogenous dispersion of GNP, GNP/PP composites were prepared by two different methods: solid state mixing (SSM) and traditional melt mixing (MM). The result shows that MM is more efficient in the dispersion of GNP particles compared to SSM method. PP nanocomposites containing only one conductive filler and two fillers were prepared at different filler concentrations. Based on the analysis of electrical and rheological properties of the prepared nanocomposites, it shows that a hybridized composite with equal amounts of GNP and CB has favorable processing properties. Conductive fibers with a core/sheath structure were produced on a bicomponent melt spinning line. The core materials of these fibers are the hybridized GNP/CB/PP nanocomposite and the sheath is pure polyamide. It was found that GNPs were separated during melt and cold drawing which results in the decrease of conductivity. However, the conductivity could partly be restored by the heat treatment. © 2013 Wiley Periodicals, Inc. J. Appl. Polym. Sci. 130: 2579–2587, 2013

KEYWORDS: conducting polymers; fibers; manufacturing; nanotubes; graphene and fullerenes; textiles

Received 2 January 2013; accepted 29 April 2013; Published online 27 May 2013

DOI: 10.1002/app.39480

INTRODUCTION

Graphene, in various forms, is a very interesting nanofiller for the preparation of conductive polymer nanocomposites. New methods for economical production of large amounts of graphite nano platelets (GNPs) consisting only of a few graphene sheets in a stack is a further motivation for the interest in GNP as a filler in electrically conductive polymer nanocomposites.[1] The mechanical properties of graphene[2,3] indicate the great potential of its use to improve properties of polymers. In order to achieve a homogenous dispersion of graphene in polymers, more or less elaborate methods to disperse graphene in polymers have been applied.[4–6] Among the different manufacturing methods, it was shown that solvent processing, elongational flow mixing and microcompounding are efficient in the dispersion and production of thin stacks of graphene in a polymer matrix.[7] However, from an industrial and environmental point of view direct melt compounding is a preferred route. Another mixing route, solid state mixing, has been proven successful for exfoliation of layered silicates in polymers.[8] Similar results are reported for GNP.[9,10] The advantage of solid state mixing is that no further preparation routes using hazardous solvent are required and that common extruders in industry can be used.

Melt spinning characteristics of carbon black (CB) and carbon nanotube (CNT) filled polyethylene (PE) and polypropylene (PP) was recently studied in order to produce textile fibers with high electrical conductivity.[11,12] Conductive fibers are interesting for various "smart textiles" applications such as heating fabrics, transfer of signals, shielding of electromagnetic radiation, and piezoelectric fibers.[13,14] Findings show that spinnability was adversely affected by the incorporation of both CB and CNT. This is related to the melt rheological properties as a result of the formation of a percolated network of carbon particles producing a strong viscosity enhancement and pronounced melt elasticity, accompanied with a yield stress phenomenon.[11,12] It was found that CB filled materials were superior to CNT counterparts being less sensitive to orientation upon melt drawing and cold drawing. Further studies revealed that fibers lost conductivity to a certain level. But the lost conductivity for the polymer/CB composites fibers could be easily restored by heat treatment, which was not the case of the polymer/CNT fibers. Still, there is a need to further improve the electrical properties of the fibers and possible ways to improve conductivity and processability could be to explore new conductive fillers and combinations of fillers.

Interestingly, Li et al.[4] recently reported a decrease in rheological response for GNP at loadings below 10 wt % in PP. It has

been shown that electrical and rheological properties are affected by combining two or three different fillers in a polymer matrix.[15–17] Filler hybridization effects have been studied for CB and CNTs in different matrixes.[17–20] Combinations of GNPs and CNTs have also been studied. A model is proposed where the CNT or CB is working as links between the GNP sheets in the conductive network.[16,21,22] In melt spinning, a large degree of orientation occur and we believe GNP will orient along the draw direction. This will result in a loss of contact points between the GNP sheets. Here, CB can work as a crosslink and increase the number of contact points.

Therefore, it is of great interest for fiber spinning purposes to investigate whether the excellent performance of CB as conductive filler can be combined with the favorable rheological and electrical properties of GNP.

In this article, we will study GNP/PP composites and hybrids of the type CB/GNP/PP. Two different manufacturing routes (melt compounding and solid state mixing) for dispersion of GNP will be evaluated. The influence of content and ratio of CB and GNP in the composites is evaluated in terms of rheological, electrical, and morphological properties. For the first time bicomponent fibers with electrical conductive CB/GNP/PP composite in the core and with a high viscosity sheath material are produced in order to understand the fillers influence on the fibers electrical properties.

EXPERIMENTAL

Materials

The polymer used for preparation of nanocomposites containing carbon particles was polypropylene (PP), grade HG265FB supplied by Borealis Group (Austria), with a density of 910 kg m^{-3}. The weight and number average molecular weights as given by the supplier are 2,11,000 and 37,800 g/mol, respectively. The melt flow index is 26 g/10 min. (2.16 kg/230°C). GNPs were obtained from XG-sciences, USA with a specific gravity of 2200 kg m^{-3}, bulk density of 30–100 kg $m^{-3}$and BET surface area 120–150 m^2 g^{-1}. Platelet thickness is 6–8 nm with an average diameter of 5 μm. All data were given by the supplier. CB was Ketjenblack 600 JD from Akzo Nobel, the Netherlands, with a specific gravity of 1800 kg m^{-3}, bulk density of 100–120 kg m^{-3} and BET surface area 1400 m^2 g^{-1}. Polyamide 6 (PA6) for production of bi-component fibers was Ultramide B33L obtained from BASF, Germany. According to the supplier the density is 1130 kg m^{-3}.

Compounding

Two different compounding methods, designated as *melt mixing* (MM) and *solid state mixing* (SSM), were used to prepare nanocomposites. In MM, PP pellets were melted in a 40 ml Brabender mixing chamber at 30 rpm for 2 min at 200°C before GNP and/or CB was added. The blend was then mixed at 100 rpm and 200°C for 10 min.

In SSM, PP pellets were first cryogenically grinded, with a 1.0 mm mesh, in a Pulverisette 14 variable speed rotor mill from Fritsch. The PP powder was dried in a vacuum oven at 80°C for 4 h to remove any moisture. PP powder and GNP were then mixed in the Brabender at 60°C at 12 rpm for 2.5 h. Temperature was then raised to 200°C. When the melting point of PP was reached the rpm was increased from 12 to 100 rpm and mixing in molten state continued for 10 min. The two routs described were used to produce compounds for production of strands and spinning trials on a capillary rheometer.

Since a larger amount of material was needed for the melt spinning of bi-component fibers a 300 ml Brabender mixing chamber was used in this case. After melting the PP pellets GNP and CB were added and compounded for 12 min at 80 rpm.

Production of Samples for Conductivity Measurements and Melt Spinning of Fibers

Fiber spinning and production of undrawn strands was performed on a CEAST Rheoscope 1000 capillary rheometer schematically shown in Figure 1. A 10 mm long capillary with a diameter (d_{cap}) of 1 mm was used. Diameter of the barrel (d_{bar}) is 9.55 mm and fibers were produced with a piston speed (v_p) of 2 mm min^{-1}. Exit velocity of the melt (v_m) is calculated to 182 mm min^{-1} using *eq.* ((1)). During spinning, the speed of the take-up wheel was gradually increased until spin line breakage occurred and the corresponding critical melt draw ratio ($MDR_{@break}$) at break was calculated using *eq.* ((2)). Distance from the capillary die to the winder was 290 mm. For production of strands a piston speed of 5 mm min^{-1} was used and strands with a length of about 15 cm were collected with a pair of tweezers. Temperature was set to 200°C in all experiments.

$$v_m = v_p \frac{d_{bar}^2}{d_{cap}^2} \quad (1)$$

$$MDR_{@break} = \frac{v_b}{v_m} \quad (2)$$

Bi-component fiber spinning was performed using a melt spinning line from Extrusion Systems Limited (ESL, Leeds, UK), schematically described in Figure 2. Details about the equipment can be found in Ref. 11.

Fibers were spun at different combinations of melt draw ratio (MDR = V_1/V_0) and solid state draw ratio (SSDR = V_3/V_2).

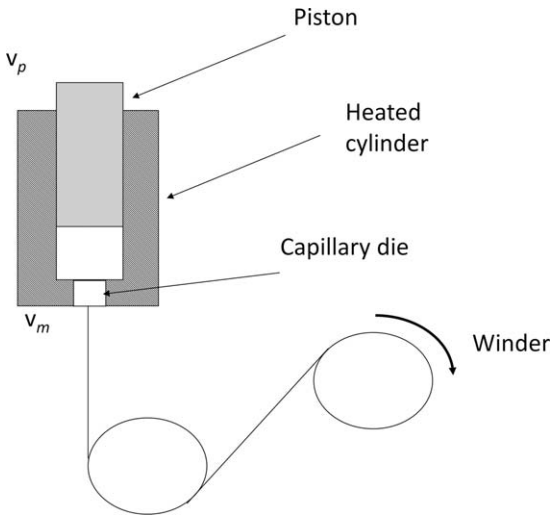

Figure 1. Schematics of rheometer for evaluation $MDR_{@break}$.

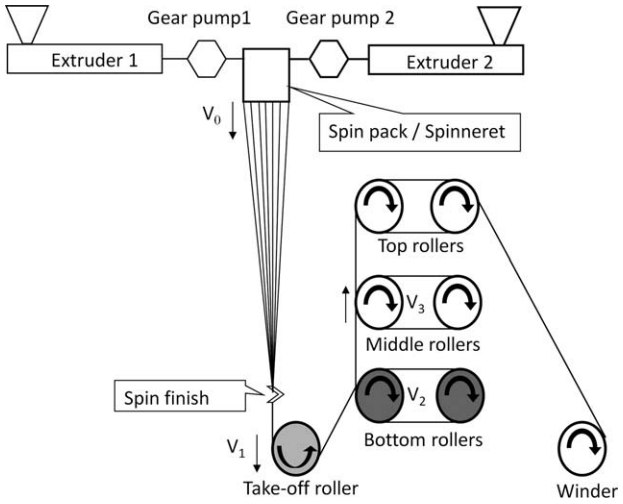

Figure 2. Schematic description of the melt spinning equipment.

The diameter of the produced fibers is controlled by the total draw ratio (MDR*SSDR) through the entire system.

PA6 was used as sheath material and GNP/CB/PP as core material with 7.5% GNP and 7.5% CB by weight. Temperature settings were as follows: Extruder 1 (sheath) zone 1, 2 and 3: 240, 260, and 270°C, respectively. Extruder 2 (core) zone 1, 2 and 3: 190, 230, and 270°C, respectively. Spinneret and metering pumps were set to 270°C.

Rheology Measurements

Dynamic rheology measurements were performed using a cone and plate rheometer (CS melt, Bohlin, Sweden). Cone diameter was 15 mm and cone angle 5.4°. Test temperature was set to 200°C. Measurements were under nitrogen atmosphere. The shear amplitude used was 1% and was checked to be within the linear viscoelastic limit.

Microscopy

Scanning electron micrographs (SEM) of extruded strands were obtained using a low vacuum JSM-6610 LV from Jeol, Japan. Micrographs of fibers were obtained using a field-emission gun SEM (FEG-SEM) JSM 7800 F from Jeol, Japan. The specimens were ion polished (Gatan model 693) to get a smooth surface for SEM observation.

Conductivity Measurements

Measurements were done using the two-probe method,[23] on un-drawn strands 100 mm long with 1 mm diameter. For bi-component fibers a bundle of fibers (~125 mm long and weight of 0.6 g) were cut with a razor blade and contacted with silver paint at the ends. The applied voltage, using a voltage supply (Oltronix D400-007D, Sweden), was varied between 20 V for low resistance samples and 120 V for high resistance samples. The current was measured with a digital multimeter (Fluke 8846A). Volume conductivity was calculated as:

$$\sigma_v = \frac{\rho l^2 I}{mU} \tag{3}$$

where ρ is the density of the core material, l is the length of the fiber bundle, I is the measured current, m is the mass of the core material, and U is the measured voltage. For each system, five specimens were employed. The relative standard deviation was below 10% for materials with conductivities higher than 10^{-4} S cm^{-1} and decreasing with increasing conductivity.

Tensile Testing of Fibers

Tensile testing of single filaments was conducted on a Vibroscope/Vibrodyn device (Lenzing, Germany). The distance between the clamps was 20 mm and test speed 20 mm min^{-1}. The results given are average of 10 samples tested.

RESULTS AND DISCUSSION

Morphology

Morphological features in extruded strands were studied by means of low vacuum SEM on ion polished surfaces cut perpendicular to the extrusion direction. GNPs, or rather stacks of GNPs, are easily recognized due to electrostatic charging. Figures 3 and 4 show micrographs of 10 wt % GNP in PP prepared by solid SSM and MM, respectively.

Several features are easily discernible. First, GNPs appear to be preferentially oriented in the extrusion direction and parallel to the surface of the strand (tangential orientation). In the central part of the strand, the tangential orientation is less pronounced (not shown in Figures 3 and 4). Second, the SSM material

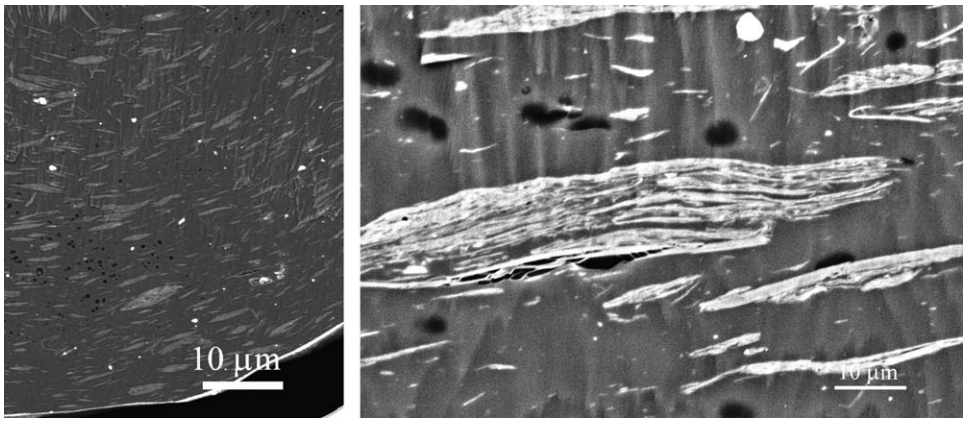

Figure 3. Scanning electron micrographs taken close to the surface of strands with 10 wt % GNP produced with SSM method low and high magnification, respectively.

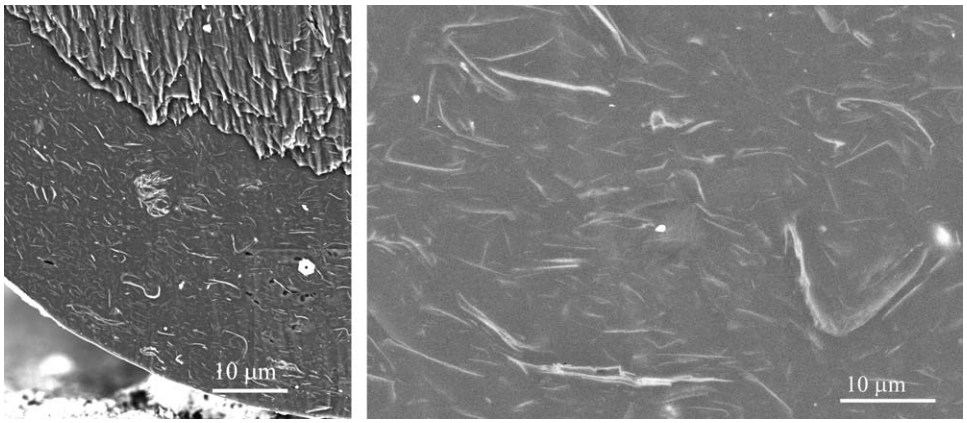

Figure 4. Scanning electron micrographs taken close to the surface of strands with 10 wt % GNP produced with MM method low and high magnification, respectively.

contains a significantly higher amount of laterally agglomerated (stacked) GNPs compared to the MM material. The MM material shows an apparent lower amount of GNPs compared to the SSM material despite the GNP concentration being the same. This may be explained by that single GNPs are not observable in SEM micrographs with the obtained resolution. Only thicker stacks of GNPs are clearly visible. We therefore believe that the MM material contain significantly more un-agglomerated GNPs with better potential to form a network of conducting particles. This is supported both by conductivity and rheological measurements to be discussed below. Further, the thinner agglomerates seen in Figure 4 appear to be less oriented and show some wrinkled and bended features. Instead of contributing to the exfoliation of GNPs the shearing process of SSM appear to have created stable stacks of GNPs more difficult to disperse into single GNPs by melt compounding. Admittedly, the total surface of PP particles to be "coated" with GNPs is very small in comparison to the surface of GNPs at 10 wt % GNP loading. The SSM process might have worked better in terms of exfoliation of GNP stacks if only very small amounts of GNP had been used. At this point, it can be noted that the surface of the extruded strands from SSM was smoother and glossier than the corresponding MM material. It is believed that the smooth surface is related to the tangential orientation of stacked GNP aggregates.

The morphology, as observed by SEM, of the CB/GNP hybrids with total carbon particle content of 10 wt % and CB/GNP weight ratios 2/8, 5/5, and 8/2 prepared by melt mixing closely resembles the morphology of pure PP/GNP composites with 8, 5, and 2 wt % GNP. The CB particles are not visible with the resolution obtained and the GNP stacks are oriented axially and tangentially in the extruded strands as in Figure 4. Since the SSM method produced more agglomerated GNPs than the MM method no trials were performed with SSM of CB/GNP hybrids.

Rheological Properties

Figure 5 shows a comparison of storage modulus for the two different mixing methods, solid state mixed, and melt mixed materials at 10 and 20 wt % GNP. It is well known that at low frequencies the storage modulus can be used to gain insight in the formation of interconnecting networks of filler particles.[7,24,25] The occurrence of a plateau at low frequency is an indication of the formation of a particle network (rheological percolation). A plateau was absent for solid state mixed samples except for 20 wt % GNP showing a slight tendency to form a plateau at the lowest angular frequencies. This can be explained by the agglomeration of GNPs into larger stacks as seen in Figure 3, leaving fewer amounts of dispersed GNPs with a large aspect ratio for network formation.

Absence of rheological percolation in the SSM material justifies that this mixing method was abandoned. The following rheological analysis is thus limited to melt mixed material only.

In Figure 6, storage modulus and the magnitude of the complex viscosity is plotted as a function of angular frequency for neat PP and its nanocomposites prepared by MM with GNP loadings of 6–20 wt %.

In Figure 6, rheological percolation is noted at 6 wt % GNP loading as evidenced by the gradual formation of a plateau at decreasing angular frequency. At lower GNP loadings, evidence of rheological percolation was not seen (not shown in Figure 6).

The behavior at higher angular frequencies is quite peculiar in that both viscosity and storage modulus is lower for the particle filled melts compared to the pure PP melt. Not until a

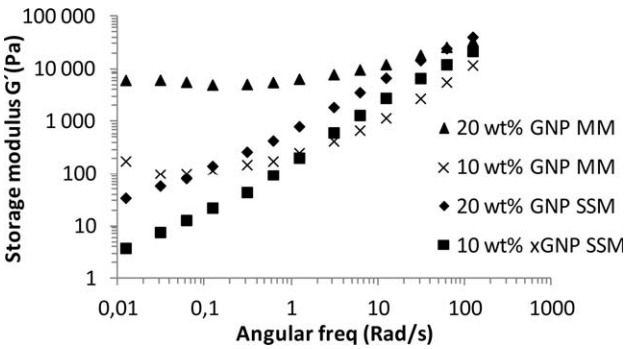

Figure 5. Comparison of storage modulus for solid state mixed (SSM) and melt mixed (MM) materials.

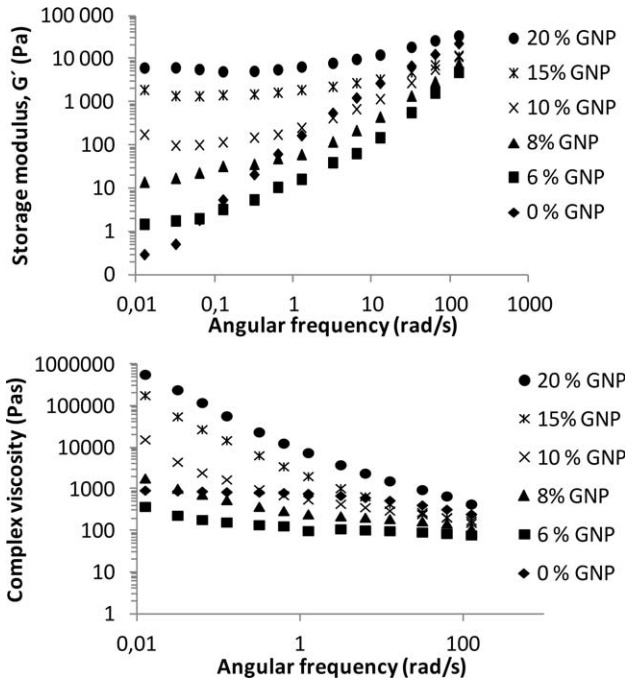

Figure 6. Storage modulus and complex viscosity plotted vs. angular frequency for melt mixed GNP composites at different loadings.

GNP loading exceeding 15 wt % the composite show a higher viscosity and modulus than the neat PP melt at high angular frequency. A similar behavior for 5 and 10 wt % GNP in PP melt was noted by Li et al.[26] using a solution/precipitation method to disperse GNP, 50–100 nm thick, in PP. The reduced viscosity compared to neat PP was referred to PP–GNP interlayer slipperiness due to a low surface friction. Kalaitzidou et al.[27] using a melt mixing method to disperse GNP, 10 nm tick, in PP saw a slightly decreased viscosity at 2 wt % GNP and a moderate increase in viscosity for 6–20 wt % GNP. The viscosity effect may thus depend on the details of used GNP and preparation method. A decreased viscosity upon addition of particles is clearly in contradiction to classical theory.[28] An obvious explanation could be that the PP matrix degrade upon the preparation of the nanocomposite (shear and high temperature during long times). However, since the preparation was done under rather mild conditions we do not think that the PP degraded in our case. Tuteja et al.[29] found a viscosity decrease (non-Einstein-like behavior) upon addition of cross linked PS nanoparticles to PS melt. This happened for very small nanoparticles (5–10 nm) with a size comparable to the hydrodynamic radius of the matrix polymer and when the number of particles was in the range of the number of PS molecules. Since the GNP particles are in the micrometer range laterally we do not think that similar mechanisms are valid in our case and prefer the interpretation of slip at the interface of GNP–PP being the cause for a reduced viscosity. In any case, the viscosity reduction upon adding GNPs to a PP melt may be advantageous in the processing to finished products of such nanocomposites. In Figure 7, storage modulus of hybrid material of CB/GNP at total filler loading of 10 wt % is plotted as function of angular frequency.

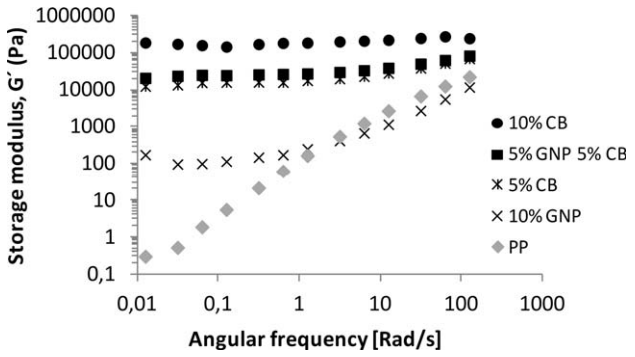

Figure 7. Storage modulus for hybrid material compared to composites with single fillers.

For comparison 5 and 10 wt % CB and 10 wt % GNP are also shown. Clearly the difference in particle shape and size of agglomerates between CB and GNP has an important impact on the rheological behavior. At equal amounts of CB and GNP, at a total concentration of 10 wt %, the storage modulus is lower than for the 10 wt % CB composite. In fact it is at the same level as a 5 wt % CB composite. Interestingly, we found a higher electrical conductivity (see below) of the hybrid (5 wt % CB and 5 wt % GNP) compared to the 5 wt % CB composite while the rheological behavior was pretty much the same of the two composites (Figure 7).

Electrical Properties

Evaluation of the electrical properties of the nanocomposites was done on undrawn strands using the two probe method as described above. As earlier mentioned two different preparation routs was applied, solid state mixing (SSM) and melt mixing (MM).

The two methods of composite preparation were found to significantly affect electrical conductivity of extruded strands. At 20 wt % GNP, the SSM show a conductivity of 7.9×10^{-6} S cm^{-1} while the MM material shows 3.8×10^{-2} S cm^{-1}. As seen in the SEM micrographs (Figure 3), of the SSM material GNPs form larger (thicker) agglomerates. As a consequence, the aspect ratio of the filler is decreased, the surface area, and the number of electrical pathways in the composite is decreased. The low conductivity of the SSM materials is paralleled by the absence of rheological percolation.

In extruded samples, the GNPs are oriented in the flow direction as is demonstrated in Figure 3. This is even more so in samples uni-axially stretched as in melt spun fibers. Orientation will significantly impair the possibility of the GNPs forming a network of conducting particles in close contact. The branched and mainly spherical morphology of high structure CB is much less prone to suffer from this effect. It is envisaged that the addition of CB could improve the conductivity by forming "bridges" between oriented GNPs or oriented stacks of GNPs and in this way produce a synergistic effect. This has been demonstrated for GNP/CB hybrid epoxy composites for which CB particles prevent GNP platelets to reform into agglomerates improving the dispersion of the GNP, This in combination with the bridging effect from the CB yield a higher electrical

Applied Polymer SCIENCE

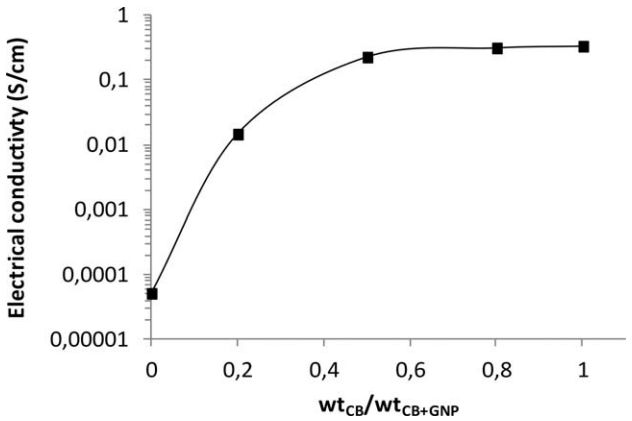

Figure 8. Variation in electrical conductivity of undrawn strands of GNP/CB/PP composites as function of a weight ratio of CB/GNP + CB (total filler content is 10 wt %).

conductivity for the hybridized composites compared to single filled materials.[30]

Bi-component fibers with 10 wt % CB in PP as core material was produced by Straat et al.[11] The variation in electrical conductivity of undrawn strands of GNP/CB/PP composites as function of the weight ratio CB/(GNP + CB) at a constant total filler content (GNP + CB) of 10 wt % is shown in Figure 8. The conductivity is increasing upon exchanging some of the GNP with CB up to a ratio of 0.5. Further increasing the amount of CB in the hybrid material has an insignificant influence on the conductivity. At equal weight fraction of CB and GNP, conductivity of the hybrid composite is 0.22 S cm^{-1}, which is slightly lower than 0.32 S cm^{-1} as measured for 10 wt % CB. From this, it is obvious that mixing the two different filler doesn't enhance the conductivity above the level of 10 wt % CB. Similar studies on GNP/CB/epoxy composites at a total filler loading of 1 wt % show that a maximum in conductivity occurs at a weight ratio CB/GNP of about 0.75.[30] This type of synergistic effect was not observed in our case (Figure 8).

The type of CB and total filler concentration with respect to the percolation threshold may be of some importance in this

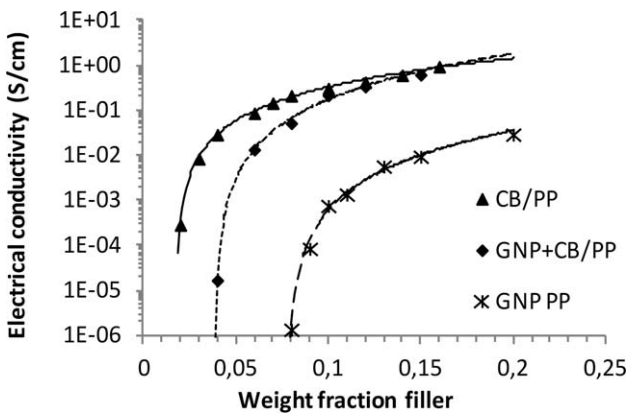

Figure 9. Electrical conductivity as function of weight fraction filler for CB, GNP + CB (ratio 1 : 1), and GNP in PP. Lines are fitted using *eq.* ((4)).

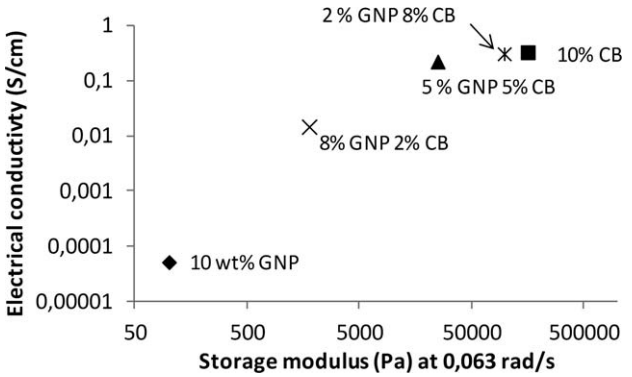

Figure 10. Electrical conductivity as function of the storage modulus at low frequency for single filled composites and hybrid composites at different filler ratio.

respect. If the conductivity of one filler is clearly superior a synergy due to network formation might not occur.

The fact that the GNP/CB/PP composite, at a weight ratio of 1 : 1 of CB : GNP has similar conductivity as the pure CB/PP composite but favorable rheological properties, as presented in Figure 7, may have significance regarding processability. Electrical conductivity for melt mixed GNP, CB and GNP/CB (ratio 1 : 1) nanocomposites at different loading of filler is shown in Figure 9.

The curves in Figure 9 represent a best fit of *eq.* (4) to the measured data.

$$\sigma = \kappa(w_f - w_c)^{\beta}. \quad (4)$$

Equation (4) is a result of classic percolation theory and is frequently used to correlate experimental data at filler loadings above the percolation threshold. In *eq.* (4) κ is related to the conductivity of the filler, w_f is weight fraction of filler, w_c is weight fraction at the percolation threshold, and β the critical exponent.[31] Values for CB/PP composites are data previously published by our group.[12] Percolation threshold for the GNP/PP, GNP/CB/PP, and CB/PP composites are about 8, 4, and 2 wt %, respectively. At 8 wt % GNP loading, the conductivity is 1.40 $\times$ 10^{-6} S cm^{-1}, Kalaitzidou et al.[27] reported a threshold at 12 wt % for a similar type of GNP (same thickness but average diameter of 15 μm instead of 5 μm) in a PP matrix prepared by melt mixing. Li et al.[4] reported a threshold of 9 wt % for even larger GNPs (thickness 50–100 nm and diameter 40–50 μm) in PP. Type of PP and GNP, process equipment and sample preparation all influence the electrical properties which may explain the differences observed.

In Figure 9, there is an intersection in conductivity between CB/PP and GNP/CB/PP at 16 wt % and above this filler loading the hybridized material have a higher conductivity.

Synergistic effects from mixing the two kinds of fillers must also be considered from a polymer processing point of view.

In Figure 10, where electrical conductivity is shown with respect to storage modulus, we find that the CB composite is having the highest value in storage modulus almost one decade higher than a GNP/CB composite with conductivity still at a similar

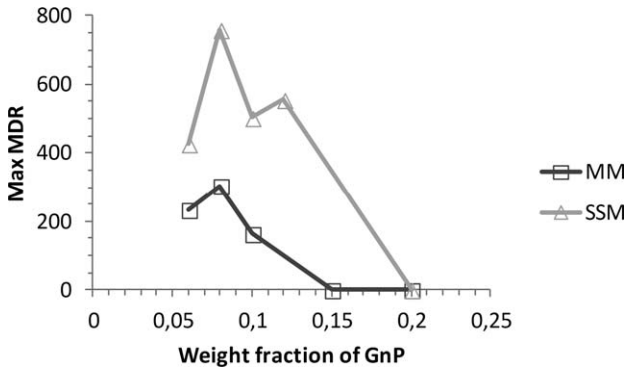

Figure 11. Comparison of $MDR_{@break}$ for MM and SSM material as function of GNP loading.

level as the CB composite. This is not quite in-line with the observation that an increase in conductivity can be directly related to a corresponding change in the rheological properties of the nanocarbon filled composite.[12,32]

We address this behavior to the particle network formed when essentially spherical CB particles and disc shaped GNP particles are mixed. The 2D shape of GNP platelets enables excellent conductivity in the direction of the platelet but not in perpendicular direction.[33] CB on the other hand has a conductivity that is independent of direction. Wei et al.[34] showed how CB particles can be dispersed on the surface of GNPs by mixing in acetone followed by stirring and sonication. A combination of the two fillers in PP can thus result in a material where GNPs can transport electrons over quite a large distance at low resistance with CB particles enabling the connection between the GNPs forming pathways for electrons. The adherence of CB particles to the GNPs will at the same time result in less contact points between CB particles so the resulting physical network is weaker which is reflected in the response of G′ while the electrical properties remain unaffected.

MELT SPINNING

Melt Draw Ratio at Break for GNP Composites Prepared by SSM and MM

Fibers were produced on a capillary rheometer as described in the experimental section. In the capillary, the polymer melt exhibit a shear deformation with a parabolic shaped velocity profile. As the melt exits, the capillary the velocity field rearranges to become flat and an extensional flow develops under the action of the applied drawing. With increasing take-up speed the strain rate increases causing a tensile stress in the polymer melt, at some level reaching a critical value resulting in fracture. The speed at which fracture occur defines the maximum melt draw ratio ($MDR_{@break}$) or spinnability.[35] A material having a $MDR_{@break}$ above 100 is to be considered as useful for fiber production.

$MDR_{@break}$ of GNP/PP composites prepared by SSM and MM methods is shown in Figure 11.

Not surprisingly, with increasing GNP concentration the spinnability decreases. This is a typical behavior of conductive polymer composites for which the rheological behavior changes from viscous to solid like.[12,36]

MM material has an $MDR_{@break}$ of 160 at 10 wt % GNP and decreasing to 0 at 15 wt % GNP while the SSM material shows a $MDR_{@break}$ of 555 at 12 wt % GNP loading. The huge difference in spinnability between MM and SSM material coincides with differences in rheological and electrical properties. The absence of a plateau in storage modulus for the SSM material seen in Figure 6, suggesting the absence of a yield stress in the material, showing similar melt behavior as PP, explains the superior spinnability of the SSM material. Since the conductivity was low even for GNP/PP prepared by MM the melt spinning of bi-component fibers was abandoned.

Melt Spinning of Bicomponent Fibers with GNP/CB Composite in the Core

Melt spinning of conductive fibers can be done by adding carbon fillers to the polymer melt. As the particles form a conductive network this also influences the melt flow behavior of the material and as a consequence the spinnability is reduced. Spin line instabilities occur when high volume loadings of small particles are introduced into the melt. Even at low MDR fiber diameter becomes irregular and as MDR increase, the amplitude of the diameter fluctuation grow and finally spin line break occur. The elongation to break is reduced as the melt exhibits a yield stress.[37] We have previously shown that this issue can be overcome by employing bi-component fiber spinning.[11,14] Here we present result from melt spinning of bicomponent yarn with sheath and core structure with PA6 as sheath material and a conductive GNP/CB/PP composite in the core. Yarns were produced according to Table I. Table II shows the properties of the produced fibers.

For fibers with a sheath/core ratio of 3/1 spin line fracture occur frequently. Fluctuations in the diameter are reflected by measured fiber titers varying from 20 to 65 dtex. Fibers could not be produced with SSDR above 1.7. To improve spinnability MDR was reduced and sheath core ratio increased. Filaments produced with SSDR 2.5 have a tenacity of 20 cN tex^{-1} which

Table I. Spinning Parameters of Bicomponent Yarns

Sample	Sheath/core volume ratio	MDR	SSDR	V_0 Spinneret (m min^{-1})	V_1 Take-off roller (m min^{-1})	V_2 Bottom roller (m min^{-1})	V_3 Middle roller (m min^{-1})
1	13/3	44	2.0	5.66	245	250	504
2	13/3	35	2.5	5.66	200	205	504
3	3/1	88	1.0	5.66	247	250	504
4	3/1	53	1.7	5.66	290	300	504

Table II. Properties of Produced Bicomponent Yarns

Sample	Conductivity (S cm^{-1})	Conductivity HT (S cm^{-1})	Titer (dtex)	Tenacity (cN tex^{-1})
1	0.023	0.143	28 ± 5.3	21.7 ± 4.0
2	0.012	0.134	30.9 ± 5.6	20.0 ± 3.5
3	0.036	0.090	40 ± 14.8	8.4 ± 3.9
4	0.014	0.138	29.4 ± 7.7	15.5 ± 3.5

is in the low range compared to commercial polyamide fibers.[38] Morphology of the fibers was studied by means of a high resolution FEG-SEM on ion polished cross sections of fibers as seen in Figures 12 and 13. Micrograph in Figure 12 shows the sheath and core structure.

The skin seen in the SEM image at the fiber surface is probably residual spin finish. The dark areas in the core are most likely entrapments of air entrained with the core material in the extruder screw. Another effect from the high viscosity of the core material is the irregular cross section of the core. As for the strands (Figures 3 and 4), GNP is preferentially oriented in the fiber direction but without tangential orientation. In Figure 13, CB primary particles appear as whitish, grape like clusters having a size around 100 nm distributed quite evenly throughout the matrix.

The GNP primary particle consists of about 10 graphene sheets with average thickness 5–10 nm[39]. The agglomerated GNPs in Figure 13 consist of more than 100 graphene sheets at a total thickness of some 100 nm. Also seen in Figure 13 are small cracks or gaps in the GNP agglomerates. During cold drawing quite strong forces are acting on the agglomerates producing some delamination between GNPs leaving gaps in the material. This kind of observation was not seen on extruded strands.

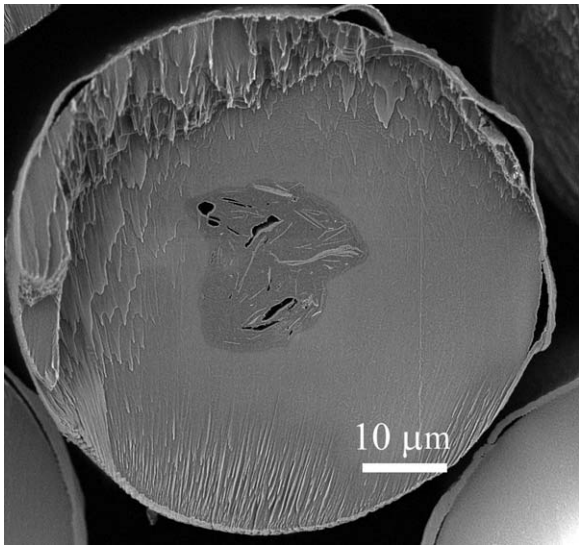

Figure 12. Scanning electron micrograph of a bicomponent filament at low magnification. The dark area in the center is the core material surrounded by a PA6 sheath.

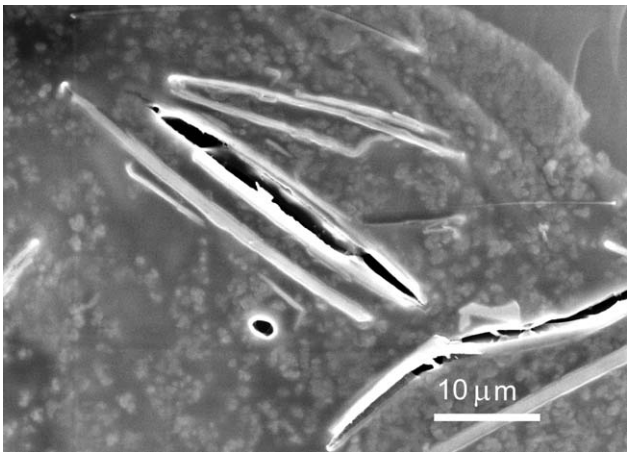

Figure 13. Scanning electron micrograph of bicomponent filament at high magnification. CB particles appear as white dots while GNP as white stripes.

The purpose of the bicomponent fiber spinning trial was to explore if GNP in combination with CB as conductive filler in the core enhances the electrical properties of the fibers. For CB filled fibers it has been shown that the loss in conductivity during cold drawing is restored by heat treatment at 180°C for 10 min.[11] In Table II, the conductivity can be partly recovered by heat treatment. However, conductivity of the heat treated yarn is 0.14 S cm^{-1} and thus far below 0.8 S cm^{-1} measured on undrawn strands of the core material. In fact, 0.14 S cm^{-1} correspond to the conductivity of an undrawn strand with 7 wt % CB. The differences in conductivity between fibers and strands can probably be related to GNP orientation during melt drawing and cold drawing. The size of the GNP particles is in the micrometer scale so the diffusion during heat treatment is limited and the gap between the particles remains too large to reform electrical pathways. CB particles are in the sub-micron scale and spherically shaped and thus believed to have a greater ability to diffuse compared to the larger disc shaped GNPs.

CONCLUSIONS

The objective of this research was to determine the effect of GNPs as filler in combination with carbon black in a PP matrix with the ultimate goal to produce electrically conductive textile fibers. For this purpose, material with CB and GNP by themselves, and in combination, were prepared and evaluated in terms of spinnability, rheological, morphological, and electrical properties. Based on the results, the following conclusions are drawn. GNP/PP composites prepared by the solid state mixing method show superior spinnability compared to traditionally melt mixed composites. However, solid state mixing creates large stacks of GNPs which results in poor electrical performance. For a hybrid composite of equal amounts of CB and GNP in a PP matrix, a slight synergistic effect in electrical conductivity takes place above a total filler amount of 16 wt %. The hybridized composite with GNP and CB show maintained electrical conductivity but a lower elastic modulus in the molten state compared to a composite with only CB at the same total filler loading. Melt spinning of a bicomponent fiber with a

GNP/CB/PP composite as core material surrounded by a PA6 sheath is demonstrated. During melt and cold drawing of the fiber conductivity is lost but could partly be restored by heat treatment. The size of the GNP is believed to limit the particle diffusion during heat treatment and the recovery of conductivity upon heating above the melting point of the polymer matrix is believed to be due to diffusion/rearrangements of CB particles reforming electrical pathways.

ACKNOWLEDGMENTS

The authors would like to thank SSF (Swedish Foundation for Strategic Research), Vinnova (The Swedish Governmental Agency for Innovation Systems) and Area of Advance: Nanoscience and Nanotechnology at Chalmers University of Technology for financial support. Mr. Lars Eklund, Swerea IVF, is acknowledged for managing the SEM equipment.

REFERENCES

1. Fukushima, H.; Graphite Nanoreinforcements in Polymer Nanocomposites, Ph.D. Thesis, Michigan State University, Michigan, **2003**.
2. Lee, C.; Wei, X.; Kysar, J. W.; Hone, J. *Science* **2008**, *321*, 385.
3. Wu, H. Multifunctional Nanocomposite Reinforced by Graphite Nanoplatelets, Ph.D. Thesis, Michigan State University, Michigan, **2011**.
4. Li, Y.; Zhu, J.; Wei, S.; Ryu, J.; Sun, L.; Guo, Z. *Macromol. Chem. Phys.* **2011**, *212*, 1951.
5. Shen, J.-W.; Chen, X.-M.; Huang, W.-Y. *J. Appl. Polym. Sci.* **2003**, *88*, 1864.
6. Zhang, H.-B.; Zheng, W.-G.; Yan, Q.; Yang, Y.; Wang, J.-W.; Lu, Z.-H.; Ji, G.-Y.; Yu, Z.-Z. *Polymer* **2010**, *51*, 1191.
7. Oxfall, H.; Rondin, J.; Bouquey, M.; Muller, R.; Rigdahl, M.; Rychwalski, R. W. *J. Appl. Polym. Sci.* **2012**; DOI:10.1002/app.38439.
8. Saito, T.; Okamoto, M. *Polymer* **2010**, *51*, 4238.
9. Wakabayashi, K.; Brunner, P. J.; Masuda, J. i.; Hewlett, S. A.; Torkelson, J. M. *Polymer* **2010**, *51*, 5525.
10. Jiang, X.; Drzal, L. T. *J. Appl. Polym. Sci.* **2012**, *124*, 525.
11. Stråål, M.; Rigdahl, M.; Hagström, B. *J. Appl. Polym. Sci.* **2012**, *123*, 936.
12. Stråål, M.; Toll, S.; Boldizar, A.; Rigdahl, M.; Hagström, B. *J. Appl. Polym. Sci.,* **2011**, *119*, 3264.
13. Tao, X. Smart Fibres, Fabrics and Clothing; Woodhead Publishing: Abington, **2001**.
14. Lund, A.; Jonasson, C.; Johansson, C.; Haagensen, D.; Hagström, B. *J. Appl. Polym. Sci.* **2012**, *126*, 490.
15. Via, M. D.; Morrison, F. A.; King, J. A.; Beach, E. A.; Wiese, K. R.; Bogucki, G. R. *Polym. Compos.* **2012**, *33*, 306.
16. Ren, P.-G.; Di, Y.-Y.; Zhang, Q.; Li, L.; Pang, H.; Li, Z.-M. *Macromol. Mater. Eng.* **2011**, *5*, 437.
17. Wen, M.; Sun, X.; Su, L.; Shen, J.; Li, J.; Guo, S. *Polymer* **2012**, *53*, 1602.
18. Via, M. D.; King, J. A.; Keith, J. M.; Bogucki, G. R. *J. Appl. Polym. Sci.* **2012**, *124*, 182.
19. Göldel, A.; Marmur, A.; Kasaliwal, G. R.; Pötschke, P.; Heinrich, G. *Macromolecules* **2011**, *44*, 6094.
20. Li, Q.; Basavarajaiah, S.; Kim, N. H.; Heo, S.-B.; Lee, J. H. *J. Appl. Polym. Sci.* **2010**, *116*, 116.
21. Kumar, S.; Sun, L. L.; Caceres, S.; Li, B.; Wood, W.; Perugini, A.; Maguire, R. G.; Zhong, W. H. *Nanotechnology* **2010**, *21*, 105702.
22. Li, J.; Wong, P.-S.; Kim, J.-K. *Mater. Sci. Eng. A* **2008**, *483–484*, 660.
23. Webster, J. G. Electrical Measurement, Signal Processing, and Displays; CRC Press: Boca Raton, **2003**.
24. Utracki, L. A. *Polym. Compos.* **1986**, *7*, 274.
25. Pötschke, P.; Bhattacharyya, A. R.; Janke, A. *Polymer* **2003**, *44*, 8061.
26. Li, B.; Zhong, W.-H. *J. Mater. Sci.* **2011**, *46*, 5595.
27. Kalaitzidou, K.; Fukushima, H.; Drzal, L. T. *Carbon* **2007**, *45*, 1446.
28. Barnes, H. A.; Hutton, J. F.; Walters, K. An Introduction to Rheology; Elsevier: Amsterdam, **1989**.
29. Tuteja, A.; Mackay, M. E.; Hawker, C. J.; Van Horn, B. *Macromolecules* **2005**, *38*, 8000.
30. Fan, Z.; Zheng, C.; Wei, T.; Zhang, Y.; Luo, G. *Polym. Eng. Sci.* **2009**, *49*, 2041.
31. Stauffer, D. Introduction to Percolation Theory; Taylor & Francis: London, **1985**.
32. Pötschke, P.; Abdel-Goad, M.; Pegel, S.; Jehnichen, D.; Mark, J. E.; Zhou, D.; Heinrich, G. *J. Macromol. Sci. A* **2009**, *47*, 12.
33. Kim, H.; Abdala, A. A.; Macosko, C. W. *Macromolecules* **2010**, *43*, 6515.
34. Wei, T.; Song, L.; Zheng, C.; Wang, K.; Yan, J.; Shao, B.; Fan, Z.-J. *Mater. Lett.* **2010**, *64*, 2376.
35. Walczak, Z. K. Processess of Fiber Formation; Elsevier: Amsterdam, **2002**.
36. Pötschke, P.; Branig, H.; Janke, A.; Fischer, D.; Jehnichen, D. *Polymer* **2005**, *46*, 10355.
37. White, J. L.; Tanaka, H. *J. Appl. Polym. Sci.* **1981**, *26*, 579.
38. Herlinger, K.-H.; Fritz, S.-G. Ullmańs Fibers; Wiley-VCH Verlag GmBh & Co.: Weinheim, **2008**.
39. Kalaitzidou, K.; Fukushima, H.; Drzal, L. T. *Compos. Part A: Appl. Sci. Manuf.* **2007**, *38*, 1675.